

Synthesis of zinc oxide nanoparticle by zinc acetate precursor and study on its catalytic properties

Azar Bagheri Ghomi*

Department of Chemistry, Center Tehran Branch, Islamic Azad University, Tehran, Iran.

Received 6 September 2015; received in revised form 27 February 2016; accepted 29 February 2016

ABSTRACT

ZnO nanoparticles have been prepared by a simple method in a short period of time. In this synthetic method, the sample was obtained using $Zn(CH_3COO)_2 \cdot 2H_2O$ and a new template of hexamine salt. Their crystalline structure and morphology were studied by XRD and SEM. The optical properties of the sample were studied by UV-visible spectroscopy. The absorption spectrum of ZnO shows that the optical band gap is 3.02 eV. In this investigation, the photocatalytic degradation of Indigo carmine(IC) in water was studied. The degradation rate is reduced as a function of increase in the initial concentration of IC. The effects of some parameters such as pH and initial concentration of dye were examined.

Keywords: Nanoparticle, ZnO, Zinc acetate, XRD, Photocatalytic.

1. Introduction

Among the various nanomaterials, ZnO nanostructures are considered to be the most promising building blocks for future electronic and optoelectronic nanodevices [1,2]. Zinc oxide (ZnO) nanomaterials, as a well-known n-type, II-IV semiconductor with a wide band gap, have aroused worldwide research interests in recent years due to their excellent optical, electrical, optoelectronic and photochemical properties [3-6]. These properties allow to envisage applications in various domains [7] ranging from ultraviolet lasing applications and catalysis [8] to optical wave guides [9] and gas sensing materials [10]. Another interest in ZnO lies in that it is one of the few oxides showing quantum confinement effects in an experimentally accessible size range [11,12]. Recently, there are several physical or chemical synthetic methods of preparing ZnO, such as thermal evaporation [13], pulsed laser deposition (PLD) [14], ion implantation [15], reactive electron beam evaporation [16], thermal decomposition [17] and sol-gel technique [18-21].

Major problems associated with industrial revolution are the depletion of nonrenewable resources, rise in global warming and the generation of harmful wastes,

which cause pollution of the environmental and damage to life forms. Semiconductor photocatalysis is intended to be both supplementary and complementary to the more conventional approaches for the destruction of hazardous chemical wastes.

To obtain ZnO nanoparticle, we chose the reflux method because of its simplicity, which offers a possibility of large-area yield at low cost. The prepared ZnO nanostructures were utilized as an efficient photocatalyst for the photocatalytic degradation of organic dye Indigo carmine under light irradiation.

2. Experimental

2.1. Material

All the compounds used were prepared from MERCK company and used without further purification. Indigo carmine was obtained from the Kimiagostar company (Iran).

Solutions were prepared by dissolving the requisite quantity of the dye in distilled water. The pH was adjusted to a given value in the range 2-10 by adding HCl (1N) or NaOH (1N) (analytical grades)

2.2. Apparatus

For the UV/photocatalyst process, irradiation was performed in a batch photoreactor of 2 liters in volume with four mercury lamps, Philips 8W (UV-C). Photo-

*Corresponding author email: azar.bagheri@iauctb.ac.ir
Tel.: +98 21 8838 5791

oxidation UV-Vis Spectrophotometer, (Shimadzu 2101) was employed for absorbance measurements using silica cells of path length 1 cm. The morphology was determined by using scanning electron microscopy (SEM) of a Holland Philips XL30 microscope. X-ray diffraction (XRD) analysis was carried out at room temperature using a Holland Philips Xpert X-ray powder diffractometer with Cu K α radiation ($\lambda=0.15406$ nm), over the 2θ collection range of $0-80^\circ$.

2.3. Preparation of ZnO

4 mmol NaOH was dissolved in 75 mL distilled water under stirring. Then, (4 mmol) the template, hexamine salt (Fig. 1), was added to the solution. Zinc acetate (1 mmol) was added to the mixture. The mixture was refluxed for 4 h in 80°C . After cooling to the room temperature, the precipitate was collected by filtration and washed with distilled water and ethanol several times. ZnO was obtained by centrifugation and drying of precipitate at room temperature.

2.4. Photocatalytic activity test

The effect of amount of ZnO nanoparticle as photocatalyst on the efficiency of photocatalytic decomposition of IC in aqueous solution was investigated. The degradation experiments were carried out in the 500 mL of 15 ppm IC. Before irradiation, the suspensions were magnetically stirred in the dark for over 30 min to ensure adsorption equilibrium of IC with the photocatalysts, and then exposed to UV light. The pH of solutions was adjusted in the range 3–10 after the addition of the catalyst. The maximum removal efficiency was obtained at pH 3. The concentration of IC was determined by measuring the absorption intensity at its maximum absorbance wavelength at 610 nm with a UV-Vis spectrophotometer.

3. Results and Discussion

3.1. Characterization of nanoparticle

The surface morphologies of the products were studied by using SEM as showed in Fig. 2. Energy dispersive spectroscopy (EDS) of prepared ZnO by wet synthesis is shown in Fig. 3. The EDX spectrum revealed that the synthesized product was quite consistent with the XRD results. The morphology of ZnO was nano sheet. X-ray powder diffraction patterns of ZnO nanoparticles are illustrated in Fig. 4. Pattern 4 was obtained from the ZnO nanoparticles prepared according to the described method.

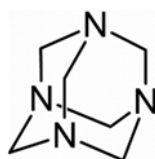


Fig. 1. Structure of hexamine salt.

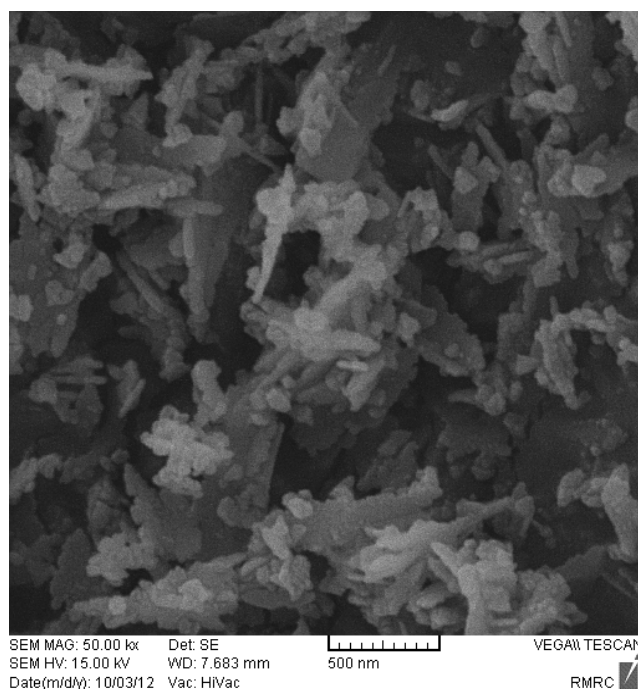


Fig. 2. SEM image of ZnO nanoparticle.

All the prominent peaks in the pattern corresponded to the wurtzite structure of ZnO, which can be indexed on the basis of JCPDS file No. 36–1451 [22]. No other characteristic peaks of the impurities are observed, indicating the high purity of the final products. These results indicate the high purity of the ZnO nanoparticles.

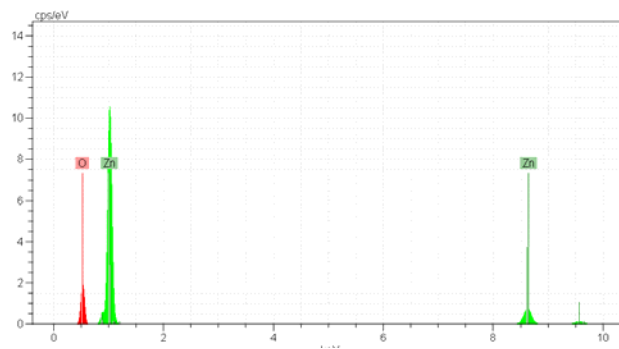


Fig. 3. EDS spectra of the ZnO.

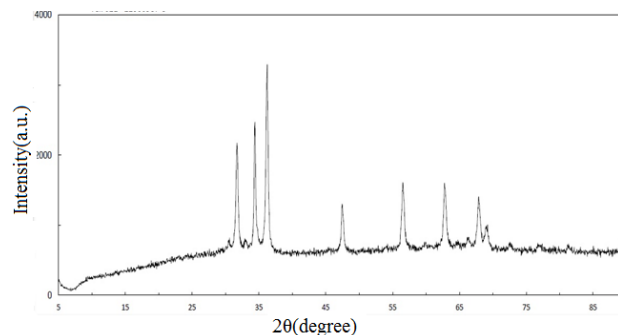


Fig. 4. X-ray diffraction pattern of ZnO.

Average crystallite sizes of products were calculated using Scherrer's formula: $D=0.9\lambda/\beta \cos \theta$ [23], where D is the diameter of the nanoparticles, λ ($\text{Cu K}\alpha$) = 1.5406 Å and β is the full-width at half-maximum of the diffraction lines. The calculated size of the crystallites of ZnO is 28 nm.

3.2. Optical properties

Absorption edge for ZnO appeared at 411 nm (Fig. 5). For analysis purposes, the diffuse reflectance, R , of the sample can be related to the Kubelka-Munk function $F(R)$ by the relation $F(R)=(1-R)^2/2R$, [24]. Adopting the method proposed by Cao et al., [25] the band-gap energies (E_g) were estimated for the ZnO. The band gap energy can be estimated on the basis of the corresponding absorption edges according to Eq. (2) [26].

$$E_g = 1240 \lambda^{-1} \quad (2)$$

Where E_g is the band-gap energy (eV) and λ is the wavelength (nm). The value of band gap energy is 3.02 eV. The calculated band gap values for ZnO are in good agreement with the literature [27,28].

3.3. Photocatalytic results

According to the results, under optimum conditions, the removal of IC was performed using ZnO nanoparticles. The decrease of absorption peaks of IC at $\lambda_{\text{max}} = 610$ nm in Fig. 6 indicates a rapid degradation of the IC. The photocatalytic activity for the ZnO was investigated after photocatalytic measurements 89% of IC was degraded for 75-min UV irradiation in the presence of nanoparticle.

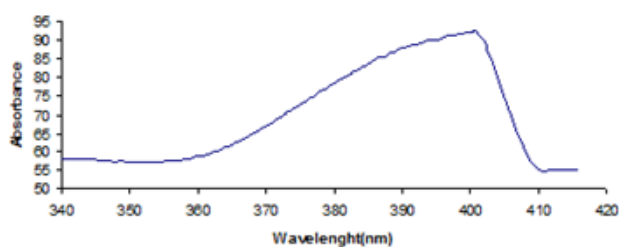


Fig. 5. Solid-state UV-Vis spectrum of ZnO.

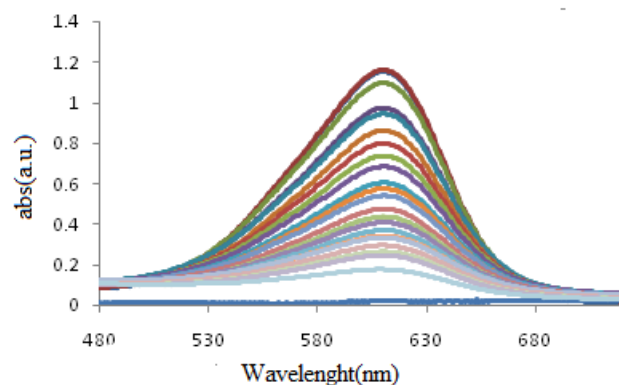


Fig.6. UV-Vis spectra of IC degradation.

The effect of initial IC concentration on the degradation efficiency was studied by varying the concentration from and keeping ZnO as constant. The degradation efficiency of IC was found to decrease with an increase in the initial dye concentration. Experiments were carried out taking different amounts of ZnO and keeping dye concentration constant. The photodegradation efficiency increases with an increase in the amount of photocatalyst, up to a value of 85 ppm and then decreases when the catalyst concentration is increased (Fig. 7).

An important factor controlling the rate of reaction that occurs on the photocatalyst surface is pH. The interpretation of pH effects on the efficiency of the photodegradation is a very difficult task because three possible reaction mechanisms can contribute to dye decolorization, namely, hydroxyl radical attack, direct oxidation by the positive hole and direct reduction by the electron in the conducting band. The importance of each one depends upon the substrate nature and pH.

4. Conclusions

The present study established that the sheet-like nanoparticles of ZnO, having diameters of 28 nm, can be prepared readily via wet chemistry by using hexamine as a template. The good quality of the obtained ZnO confirms the high prospects of our process compared to the previous studies [29-35]. The particle size determines the specific surface area and hence the number of active surface sites where the photogenerated charge carriers can undergo interfacial transfer and react with adsorbed molecules. The smaller crystallite size leads to the larger band gap and higher photodecolorization.

In the present study, the efficiency of photocatalytic degradation of IC dye solution was studied using prepared crystalline ZnO composite by suspending in aqueous media in presence of light. The results indicated that degradation efficiency of synthesized ZnO nanoparticles was affected by irradiation time, dye solution pH and catalyst concentration. The synthesized ZnO is considered the most suitable for photocatalytic degradation.

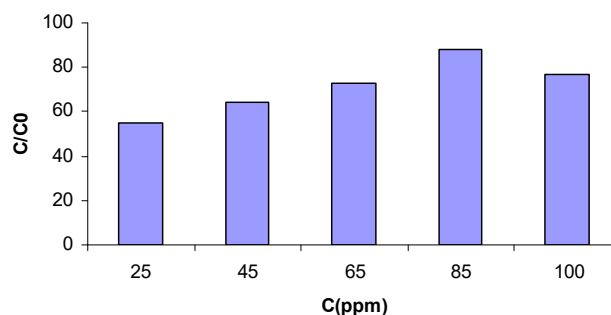


Fig 7. Effect of photocatalyst concentration on % dye solution degradation (irradiation time = 60 min, pH=3).

Acknowledgment

We would like to thank the Islamic Azad University Center Tehran Branch for its invaluable support throughout the project.

References

- [1] Ü. Özgür, Y.I. Alivov, C. Liu, *J. Appl. Phys.* 98 (2005) 301-305.
- [2] D. Panda, T.Y. Tseng, *J. Mater. Sci.* 48 (2013) 6849–6877.
- [3] P.D. Yang, H.Q. Yan, *Adv. Funct. Mater.* 12 (2002) 323–331.
- [4] J. Safari, S. Gandomi-Ravandi, Z. Akbari, *Iranian J. Catal.* 3 (2013) 149-155.
- [5] H. Faghihian, A. Bahrnifard, *Iran. J. Catal.* 1 (2011) 45-50.
- [6] M.H. Habibi, E. Askari, *Iran. J. Catal.* 1 (2011) 41-44.
- [7] G.C. Yi, C.R. Wang, *Semicond. Sci. Technol.* 20 (2005) 522–534.
- [8] T. Fujitani, J. Nakamura, *Catal. Lett.* 56 (1998) 119–124.
- [9] E.L. Paradis, A.J. Shuskus, *Thin Solid Films* 38 (1976) 131–141.
- [10] L.C. Tien, P.W. Sadik, *Appl. Phys. Lett.* 87 (2005) 222106–222108.
- [11] U. Koch, A. Fojtik, *Chem. Phys. Lett.* 122 (1985) 507–510.
- [12] T. Masaki, S.J. Kim, H. Watanabe, *J. Ceram. Process Res.* 4 (2003) 135–139.
- [13] L. Chen., Z.Q. Chen., X.Z. Shang, *Solid State Commun.* 137 (2006) 561–565.
- [14] Z.L. Wang, *J. Phys. Condens. Matter.* 16 (2004) 829–858.
- [15] H.Z. Wu, D.J. Qiu, Y.J. Cai, *J. Cryst. Growth* 245 (2002) 50–55.
- [16] L.L. Yang, J.H. Yang, X.Y. Liu, *J. Alloys. Compd.* 463 (2008) 92–95.
- [17] L. Spanhel, M.A. Anderson, *J. Am. Chem. Soc.* 113 (1991) 2826–2833.
- [18] E.A. Meulenkamp, *J. Phys. Chem. B* 102 (1998) 5566–5572.
- [19] Y.L. Wu, A.I. Y. Tok, F.Y.C. Boey, *Appl. Surf. Sci.* 253 (2007) 5473–5479.
- [20] L. Guo, S.H. Yang, C.L. Yang, *Appl. Phys. Lett.* 76 (2000) 2901–2903.
- [21] Y.H. Tong, Y.C. Liu, S.X. Lu, *J. Sol. Gel. Sci. Technol.* 30 (2004) 157–161.
- [22] Q.S. Kong, X.L. Wu, *Acta. Phys. Chim. Sin.* 24 (2008) 2179.
- [23] M.E. Fragalà, Y. Aleeva, G. Malandrino, *Thin Solid Films* 519 (2011) 7694–7701.
- [24] G. Kortum, *Reflectance Spectroscopy*, Springer-Verlag, New York, 1969.
- [25] G. Cao, L.K. Rabenberg, C.M. Nunn, T.E. Mallouk, *Chem. Mater.* 3 (1991) 149-156.
- [26] S.B. Khan, M. Faisal, *Talanta* 85 (2011) 943–949
- [27] P. Muthukumara, T.M. Selvakumarib, S. Ganesan, *Dig. J. Nanomater Bios.* 5 (2010) 635-639.
- [28] F.I. Ezema, U.O.A. Nwankwo, *Dig. J. Nanomater Bios.* 5 (2010) 981-987.
- [29] N.F. Hamedania, A. Mahjoub, A. Khodadadib, Y. Mortazavic, *Sensors Actuators B* 156 (2011) 737-742.
- [30] N. Talebian, S.M. Amininezhad, M. Doudi, *J. Photochem. Photobiol. B* 120 (2013) 66-73.
- [31] G. Bandekar, N.S. Rajurkar, I.S. Mulla, U.P. Mulik, *Appl. Nanosci.* 4 (2014) 199-208.
- [32] C. Shiyan, Z. Bihui, H. Weili, *Carbohydr. Polymers* 92 (2013) 1953-1959.
- [33] M. Thirumavalavan, F. Yang, J. Lee, *Environ. Sci. Pollut. Res.* 20 (2013) 5654-5664.
- [34] T. Thilagavathi, D. Geetha, *Appl. Nanosci.* 3 (2013) 141-144.
- [35] G. Dutta, *J. Nanobiotechnol.* 10 (2012) 29-35.